Int. J. Heat Mass Transfer. Vol. 29, No. 3, pp. 439–449, 1986
Printed in Great Britain

0017–9310/86 $3.00 + 0.00
Pergamon Press Ltd.

Numerical study of two-dimensional natural convection in a horizontal fluid layer heated from below, by finite-element method: influence of Prandtl number

HENRI BERTIN and HIROYUKI OZOE

Department of Industrial and Mechanical Engineering, Okayama University, Tsushima, Okayama 700, Japan

(*Received* 26 *June* 1985 *and in final form* 23 *August* 1985)

Abstract—Natural convection in a two-dimensional horizontal fluid layer heated from below and cooled from above was computed by a finite-element method using a Galerkin approach. In the case of $Pr = 10$ the Nusselt number, obtained by an extrapolation to zero element size, agreed well with the experimental data of Silveston [*Forsch. Ing.* **24**, 59–69 (1958)], for a range of Rayleigh numbers from the critical value up to 25,000. For the Prandtl numbers varying from 0.001 to 1000, steady-state solutions for convection, heat transfer rates and the critical Rayleigh numbers were computed. A correlating equation for critical Rayleigh number as a function of Prandtl number was proposed. Using the correlating equation of Malkus and Veronis [*J. Fluid Mech.* **4**, 225–260 (1958)], it was possible to compute the heat transfer rate near the critical state, for every Prandtl number higher than 0.001.

1. INTRODUCTION

AFTER the works by Bénard and Rayleigh, there are many studies dealing with the critical condition for the onset of instability in an horizontal layer of fluid of infinite extent heated from below.

The width of the roll cell in an infinite horizontal fluid layer between two rigid walls, heated from below and cooled from above has been studied by a number of papers [1]. However, there appears to be no definitive agreement on the stable width of a roll cell. Linear stability analysis at infinite Prandtl number suggests the critical wave number $a_c = 3.117$, which indicates a square roll cell. Ozoe *et al.* [2] reported numerical calculations with various roll widths but no definitive conclusion can be drawn on the stable width of a roll cell. In accordance with experimental observations [3] the motion of fluid, just above the critical state, is postulated to be a series of identical square roll cells with parallel axes. In that case, the theoretical value for the critical Rayleigh number is 1707.8.

When the Prandtl number becomes low, less than 0.1, say, the non-linear inertial terms can not be neglected. In that case, natural convection is known to depend on the Prandtl number, Pr, as well as on the Rayleigh number, Ra. There have been only a few experimental investigations dealing with the determination of the critical Rayleigh number Ra_c for low Prandtl number. Such low values occur only for liquid metals such as mercury ($Pr = 0.025$) and sodium, and in astrophysical applications. Experiments with these fluids are very difficult to perform, but some results are available for mercury. Verhoeven [4] determined a value of 1808 $\pm$16 for the critical Rayleigh number of mercury in a cylinder. Soberman [5] observed critical Rayleigh numbers as high as 2000 and as low as 1200 for mercury.

For the dependence of the critical Rayleigh number on the Prandtl number, Samels and Churchill [6] developed finite-difference solutions for two-dimensional natural convection in long, rectangular channels heated from below. Their computed results indicate a dependence on Pr for Pr less than 0.1, and their plots of the Nusselt number Nu vs Ra for different Pr extrapolate to different values of Ra_c. Chao *et al.* [7] carried out finite-difference computations for the dependence of the critical Rayleigh number on the Prandtl number and correlated their results with the expression

$$Ra_c = 1707.8[1+(0.00717/Pr)^{5/3}]^{3/5}. \quad (1)$$

In the present work, the finite-element method was used to compute natural convection in a horizontal, infinite layer of fluid heated from below and cooled from above. First, the rate of heat transfer was investigated for the Rayleigh numbers up to 25 000 with a Prandtl number of 10, and then the influence of the Prandtl number over the range of 0.001 to 1000, on the critical Rayleigh number.

2. MATHEMATICAL MODEL

An infinitely long, two-dimensional roll cell with a square cross section [3], was postulated, as shown in Fig. 1. The equations for the conservation of mass, momentum and energy were accordingly expressed as

$$\frac{\partial u}{\partial x}+\frac{\partial v}{\partial y}=0 \quad (2)$$

$$u\frac{\partial u}{\partial x}+v\frac{\partial u}{\partial y}=\left(\frac{-1}{\rho}\right)\frac{\partial P}{\partial x}+\nu\left(\frac{\partial^2 u}{\partial x^2}+\frac{\partial^2 u}{\partial y^2}\right) \quad (3)$$

NOMENCLATURE

a_c	critical wave number	u	velocity in x-direction
$[A]$	matrix $(N \times N)$	U	dimensionless velocity
$[A']$	matrix $(N \times N)$	v	velocity in y-direction
B	constant (Malkus and Veronis equation)	V	dimensionless velocity
		x	horizontal coordinate
$\{B\}$	RHS vector	X	dimensionless coordinate
b	exponent (correlating equation)	y	vertical coordinate
C	constant (correlating equation)	Y	dimensionless coordinate.
C_p	specific heat		
Gr	Grashof number, Ra/Pr	Greek symbols	
g	acceleration due to gravity	α	thermal diffusivity
H	height and width of roll cell	β	thermal coefficient expansion
k	thermal conductivity	δe	triangular element
$L1, L2, L3$	interpolating functions	Δ_e	area of element δe
Nu	Nusselt number	ΔT	temperature difference, $T_1 - T_2$
N	total number of node points	Δr	grid size
$\{N1\}$	cardinal basis	μ	viscosity
$\{N1\}^t$	transpose of $\{N1\}$	ν	kinematic viscosity
n	exponent (correlating equation)	ρ	density
P	pressure	ρ_0	density at T_0
Pr	Prandtl number, ν/α	θ	temperature perturbation
Ra	Rayleigh number	ψ	dimensionless streamfunction
Ra_c	critical Rayleigh number	Φ	dimensionless temperature
T	temperature	Ω	dimensionless vorticity.

$$u\frac{\partial v}{\partial x} + v\frac{\partial v}{\partial y} = \left(\frac{-1}{\rho}\right)\frac{\partial P}{\partial y} + \nu\left(\frac{\partial^2 v}{\partial x^2} + \frac{\partial^2 v}{\partial y^2}\right) + \rho g \quad (4)$$

$$\rho C_p\left(u\frac{\partial T}{\partial x} + v\frac{\partial T}{\partial y}\right) = k\left(\frac{\partial^2 T}{\partial x^2} + \frac{\partial^2 T}{\partial y^2}\right). \quad (5)$$

The well-known Boussinesq approximation is employed, i.e. that physical properties are constant except for the density ρ in the buoyancy term, which is assumed to vary with temperature only according to

$$\rho = \frac{\rho_0}{1+\beta(T-T_0)} \quad (6)$$

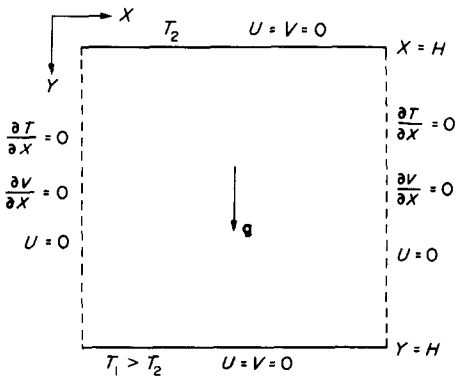

FIG. 1. Physical geometry and boundary conditions.

where

$$\beta = -\left[\frac{1}{\rho}(\partial\rho/\partial T)\right]_{T_0} \quad (7)$$

is the coefficient for thermal expansion.

Taking the cross derivatives of the two equations of motion and subtracting to eliminate the pressure term, then, after dedimensionalizing, introducing the streamfunction and vorticity gives

$$\frac{\partial^2\Phi}{\partial X^2} + \frac{\partial^2\Phi}{\partial Y^2} = U\frac{\partial\Phi}{\partial X} + V\frac{\partial\Phi}{\partial Y} \quad (8)$$

$$\frac{\partial^2\Omega}{\partial X^2} + \frac{\partial^2\Omega}{\partial Y^2} = \frac{1}{Pr}\left(U\frac{\partial\Omega}{\partial X} + V\frac{\partial\Omega}{\partial Y}\right) + Ra\frac{\partial\Phi}{\partial X}. \quad (9)$$

Here Φ, Ω, U, V, X and Y are the non-dimensionalized values for temperature, vorticity and components of the velocity, and X and Y are the coordinates.

Also

$$\Omega = -\nabla^2\psi = \frac{\partial V}{\partial X} - \frac{\partial U}{\partial Y} \quad (10)$$

where ψ is the streamfunction

$$U = \partial\psi/\partial Y \quad \text{and} \quad V = -\partial\psi/\partial X \quad (11)$$

also

$$Pr = \nu/\alpha \text{ (Prandtl number)} \quad (12)$$

$$Ra = C_p\rho_0^2 H^3 g\beta\Delta T/\mu k \text{ (Rayleigh number)} \quad (13)$$

$$\Phi = (T - T_0)/\Delta T, \quad T_0 = (T_1 + T_2)/2. \tag{14}$$

The revised boundary conditions are

$$X = 0, 1: \quad \psi = \Omega = 0; \quad \partial\Phi/\partial X = 0 \tag{15}$$

$$Y = 0: \quad \psi = 0; \quad \Omega = -\partial U/\partial Y; \quad \Phi = -1/2 \tag{16}$$

$$Y = 1: \quad \psi = 0; \quad \Omega = -\partial U/\partial Y; \quad \Phi = 1/2. \tag{17}$$

The vorticity on the wall can be computed from the streamfunction as follows:

$$\Omega = -\partial U/\partial Y = -\partial^2\psi/\partial Y^2. \tag{18}$$

For a low Prandtl number, the temperature profile is expected to be nearly linear. Therefore the temperature can be assumed to be the sum of a conduction term and a perturbation term as per Chandrasekhar [1]:

$$\Phi = \Phi_c + \theta \tag{19}$$

where

$$\Phi_c = Y - 0.5 \text{ (profile due to conduction only)} \tag{20}$$

and θ is a perturbation of the temperature from the state of pure conduction.

Next an equation employed by Chao *et al.* [7] was used to study the influence of a low Prandtl number. The perturbation for temperature yields the following set of equations:

$$\frac{1}{Pr}\left(\frac{\partial^2\theta}{\partial X^2} + \frac{\partial^2\theta}{\partial Y^2}\right) = U\frac{\partial\theta}{\partial X} + V\frac{\partial\theta}{\partial Y} + V \tag{21}$$

$$\frac{\partial^2\Omega}{\partial X^2} + \frac{\partial^2\Omega}{\partial Y^2} = U\frac{\partial\Omega}{\partial X} + V\frac{\partial\Omega}{\partial Y} + Gr\frac{\partial\theta}{\partial X} \tag{22}$$

where $Gr = Ra/Pr$, is the Grashof number.

However, this formulation did not yield a convergent result for Pr less than 0.01 and a formulation which yielded the following alternative set of equations was employed:

$$\frac{1}{Pr\sqrt{Gr}}\left(\frac{\partial^2\theta}{\partial X^2} + \frac{\partial^2\theta}{\partial Y^2}\right) = U\frac{\partial\theta}{\partial X} + V\frac{\partial\theta}{\partial Y} + V \tag{23}$$

$$\frac{1}{\sqrt{Gr}}\left(\frac{\partial^2\Omega}{\partial X^2} + \frac{\partial^2\Omega}{\partial Y^2}\right) = U\frac{\partial\Omega}{\partial X} + V\frac{\partial\Omega}{\partial Y} + \frac{\partial\theta}{\partial X}. \tag{24}$$

The boundary conditions on the perturbation of the temperature correspond to no perturbation on the wall, i.e.

$$Y = 0, \quad 1 \to \theta = 0. \tag{25}$$

3. FINITE-ELEMENT FORMULATION

Most of the investigations of convection with the finite-element method deal with two-dimensional motion in a rectangular channel heated on one vertical wall and cooled on the opposing wall. As a first try, the equations (8) and (9) were interpreted as Poisson equations after Tabarrok and Lin [8] for the vertical configuration, and Ozoe *et al.* [9] for the horizontal one. Both of these investigations used a variational method to solve the problem with the convective term being approximated by its value at the gravitational center of each element. Their results were limited to Rayleigh numbers less than 3000 for the horizontal configuration.

Since equations (8) and (9) are nonlinear, an exact variational formulation corresponding to this kind of equation is not possible.

There are several possible methods of solving these equations. The popular schemes are those of the weighted residuals with least squares, collocation method and the Galerkin method. Ikenouchi *et al.* [10] used the Galerkin method to solve the Navier–Stokes equations, and more recently Moult *et al.* [11] solved several two-dimensional steady flow problems by the Galerkin method.

3.1. *Method of weighted residuals*

The Galerkin approach was used in the present investigation. Detailed explanations of the use of this method in fluid mechanics are given in books such as Zienkiewicz [12], Chung [13] and Baker [14].

3.2. *Energy equation*

Equation (8) yields the following Galerkin integral:

$$\int\int_{\delta e} \{W(X,Y)\}\left(-\frac{\partial^2\Phi}{\partial X^2} - \frac{\partial^2\Phi}{\partial Y^2} + U\frac{\partial\Phi}{\partial X} + V\frac{\partial\Phi}{\partial Y}\right) dX\, dY = 0 \tag{26}$$

where $\{W(X,Y)\}$ is a complete, linearly independent set of weighting functions.

The temperature, vorticity and streamfunction can be approximated as the product of a shape function and the nodal values:

$$\Phi(X,Y) = \{N1(X,Y)\}^t\{\Phi\}_e \tag{27}$$

$$\Omega(X,Y) = \{N1(X,Y)\}^t\{\Omega\}_e \tag{28}$$

$$\psi(X,Y) = \{N1(X,Y)\}^t\{\psi\}_e \tag{29}$$

where $\{N1(X,Y)\}$ is a (1×3) row matrix of the interpolating function for each triangular element (shape function). $\{\Phi\}_e$, $\{\Omega\}_e$ and $\{\psi\}_e$ are the values of the temperature, vorticity and streamfunction at the vertices of the element.

The details of the calculation and derivation of the shape functions $\{N1(X,Y)\}$ can be found in Zienkiewicz [12] and Baker [14].

It is possible to substitute the set of shape functions for the set of weight functions in the Galerkin integral of equation (26)

$$\int\int_{\delta e} \{N1(X,Y)\}\left(-\frac{\partial^2\Phi}{\partial X^2} - \frac{\partial^2\Phi}{\partial Y^2} + U\frac{\partial\Phi}{\partial X} + V\frac{\partial\Phi}{\partial Y}\right) dX\, dY = 0 \tag{30}$$

The Green–Gauss theorem is used to transform the second derivatives:

$$\int\int_{\delta e} \{N1(X,Y)\}\frac{\partial^2\Phi}{\partial X^2}\,dX\,dY = -\int\int_{\delta e}\frac{\partial\{N1(X,Y)\}}{\partial X}\frac{\partial\Phi}{\partial X}\,dX\,dY + \oint_{\sigma}\{N1(X,Y)\}\frac{\partial\Phi}{\partial X}\,d\sigma. \quad (31)$$

The boundary conditions (Φ = constant or $\partial\Phi/\partial X = 0$), require the second integral of the RHS to vanish identically on the boundaries. In consequence, the Galerkin integral becomes

$$\int\int_{\delta e}\left(\{N1\}U\frac{\partial\{N1\}^t}{\partial X}\{\Phi\}_e + \{N1\}V\frac{\partial\{N1\}^t}{\partial Y}\{\Phi\}_e + \frac{\partial\{N1\}}{\partial X}\frac{\partial\{N1\}^t}{\partial X}\{\Phi\}_e + \frac{\partial\{N1\}}{\partial Y}\frac{\partial\{N1\}^t}{\partial Y}\{\Phi\}_e\right) \times dX\,dY = \{0\}. \quad (32)$$

The values of U and V are considered to be constant on each element. Of course it is possible to consider the velocity components in terms of the streamfunction, but that requires the solution of a nonlinear system. In consequence, schemes such as that of Newton and Raphson, which makes the solution scheme much more complicated, are required.

Consider one term of the Galerkin integral:

$$\int\int_{\delta e}\left(\{N1\}U\frac{\partial\{N1\}^t}{\partial X}\{\Phi\}_e\right)dX\,dY = U\int\int_{\delta e}\{N1\}\frac{\partial\{N1\}^t}{\partial X}\{\Phi\}_e\,dX\,dY \quad (33)$$

$\{N1(X,Y)\}$ is a (1×3) row matrix, $\partial\{N1(X,Y)\}^t/\partial X$ is a (3×1) line matrix and the product is a (3×3) square matrix.

The following formula for integration [12] can be used:

$$\int\int_{\delta e} L_1^a L_2^b L_3^c\,dX\,dY = [(a!\,b!\,c!)/(a+b+c+2)!]2\Delta_e \quad (34)$$

where Δ_e is the area of the triangle δe and Li are the interpolating functions.

The expression of the Galerkin integral is, for each triangular element, a (3×3) square matrix. The global stiffness matrix is obtained by combining these elementary matrices on the domain. The result to be solved is now a linear system.

$$[A]\{\Phi\} = \{B'\} \quad (35)$$

where $[A]$ is an $(N\times N)$ square matrix, and $\{\Phi\}$ is an N vector representing the values of temperature at every vertex. $\{B'\}$ is determined by the boundary conditions.

3.3. *Equation for vorticity transport*

The same method is used for the vorticity transport equation as for the energy equation.

The temperature gradient in the equations (9), (22) or (24) is considered as a constant in every step. In consequence, a linear system is obtained

$$[A']\{\Omega\} = \{B\} \quad (36)$$

where $\{B\}$ on the RHS is a function of the temperature gradient.

3.4. *Streamfunction equation*

The relationship between the vorticity and streamfunction

$$\nabla^2\psi = -\Omega \quad (37)$$

is a typical Poisson equation and can be solved by a variational formulation.

4. FINITE-ELEMENT ALGORITHM

The square cross-section of the roll cell is divided into a number of triangles as shown in Fig. 2. The boundary conditions are also shown in that figure.

If the same shape elements are chosen, as indicated on Fig. 2, the elementary matrix corresponding to the Galerkin integral is the same for each element.

The computations were carried out as follows. The motion was postulated to be a long roll cell with normal axis, *Ra* being near the critical value of 1708. The computations were started by imposing a shock in temperature, i.e. a weak symmetrical perturbation in temperature to initialize the motion. The vorticity and streamfunction corresponding to the initial field of the perturbed temperature was then computed. The vorticity on the wall must be computed as follows:

$$\Omega = -\partial^2\psi/\partial Y^2 = -2\psi_1/(\Delta r)^2 \quad (38)$$

here ψ_1 is the value of the streamfunction one grid space away from the wall.

The computation is continued to convergence for one set of *Ra* and *Pr* numbers. It is then possible to increase the Rayleigh number and iterate to convergence.

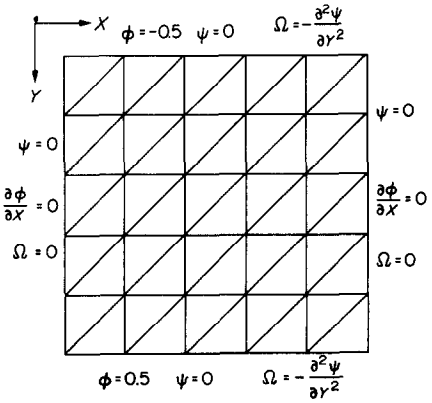

FIG. 2. Finite-element grid and revised boundary conditions.

At every step of the computation, the temperature field, vorticity, streamfunction and vorticity on the wall were computed successively. The average Nusselt number at the cooled plate was calculated from a second-order Taylor series for temperature field.

$$Nu = \int_0^1 (\partial\Phi/\partial Y)_{Y=0}\,dX$$

$$= \int_0^1 (-3\Phi_w + 4\Omega_{\Delta r} - \Phi_{2\Delta r})/2\Delta r)\,dX. \quad (39)$$

The number of iteration at every step depends on the grid size, the Rayleigh and the Prandtl numbers and varied from 15 to 150. To avoid numerical instability, for small grid sizes, it was necessary to use the average value of the two previous steps.

5. NUMERICAL RESULTS

Three sets of equations were used to study the influence of the Prandtl number: (8), (9); (21), (22) and (23), (24). In each case, three grid sizes were used: (6 × 6), (10 × 10) and (14 × 14) for the higher Prandtl numbers; and (10 × 10), (14 × 14) and (18 × 18) for the lower ones.

The convergence of the solution was monitored by the Nusselt number. For example, Fig. 3 shows the variation of the Nusselt number as a function of the iteration number for $Pr = 10$ and a grid size of (10 × 10). The increment in the Rayleigh number was 500. An oscillatory response can be observed before convergence. For low Prandtl numbers, a smaller Rayleigh number increment of 100 was required to obtain convergence. Figure 4 shows the response of the Nusselt number for $Pr = 0.01$ and a (18 × 18) grid number.

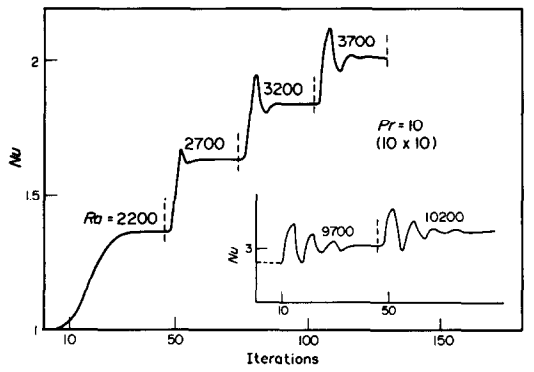

FIG. 3. Convergence of the Nusselt number for increasing Rayleigh number ($Pr = 10.0$, 10 × 10 divisions).

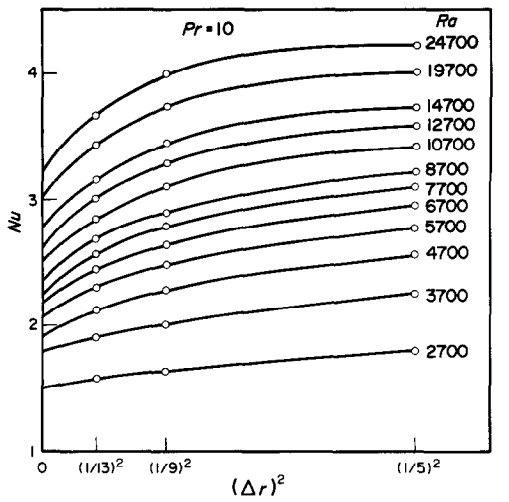

FIG. 5. Extrapolation of Nusselt numbers to zero grid size ($Pr = 10.0$).

The results for different grid sizes can be used as proposed by Churchill *et al.* [15] for finite differences, to obtain the Nusselt number to zero grid size, by plotting against $(\Delta r)^n$, where n is the order of the truncation error. Figures 5 and 6 show the results of this procedure for $Pr = 10$ and $Pr = 0.01$ and $n = 2$.

Our results for $Pr = 10$ are compared with the experimental data of Silveston [16] in Fig. 7; good agreement is obtained particularly for the lower Rayleigh numbers. The numerical results and extrapolated values of the Nusselt number for $Pr = 10$ are summarized in Table 1.

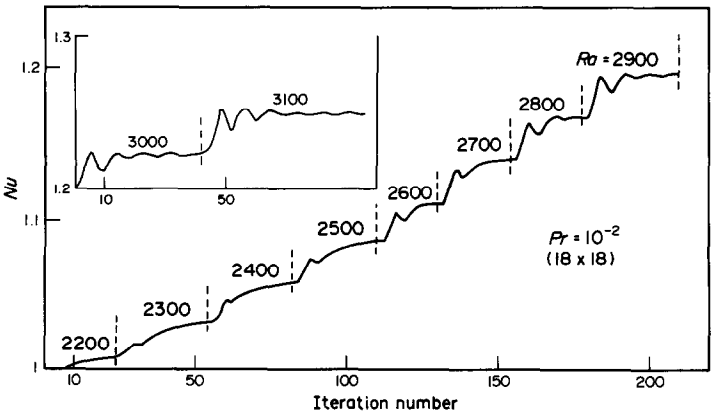

FIG. 4. Convergence of the Nusselt number for increasing Rayleigh number ($Pr = 0.01$, 18 × 18 divisions).

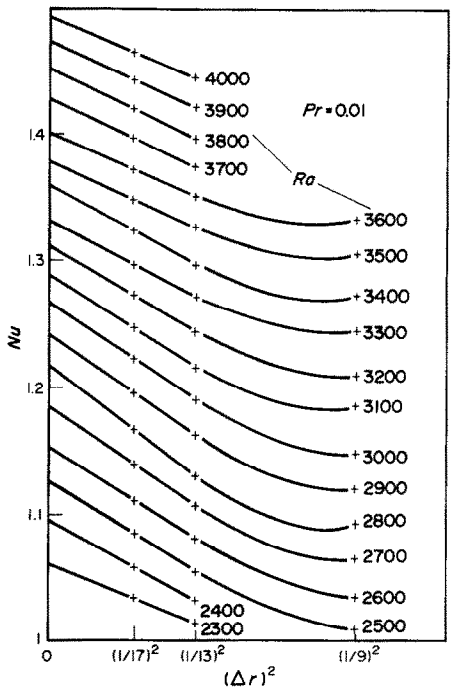

FIG. 6. Extrapolation of Nusselt numbers to zero grid size ($Pr = 0.01$).

Table 2 lists the computed and extrapolated values of the Nusselt number for $Pr = 0.01$, and Table 3 the extrapolated values of the Nusselt number for several Prandtl and Rayleigh numbers. These results are plotted in Fig. 8. Computed contours of isotherms and streamfunction corresponding to $Ra = 3000$ are in Figs. 9–11 for $Pr = 10$, 0.1 and 0.01, respectively. The grid size is (14 × 14) for all cases and the Nusselt number is equal to 1.6871 ($Pr = 10$, Fig. 9), 1.5472 ($Pr = 0.1$, Fig. 10) and 1.1903 ($Pr = 0.01$, Fig. 11), respectively.

5.1. *Critical Rayleigh number*

The critical Rayleigh number determined was obtained by extrapolation of the computed values to the conductive state ($Nu = 1$) by plotting $Nu - 1$ vs $1/Ra$ (Fig. 12) as per the correlating equation of Malkus and Veronis [17]:

$$Nu = 1 + B(1 - Ra_c/Ra). \quad (40)$$

The values of the critical Rayleigh number obtained in this way were:

$Pr = 0.003$ $\quad Ra_c = 2392.$

$Pr = 0.01$ $\quad Ra_c = 2095.$

$Pr = 0.025$ $\quad Ra_c = 1894.$

$Pr = 0.1$ $\quad Ra_c = 1721.$

$Pr = 1.0$ $\quad Ra_c = 1712.$

$Pr = 1000.$ $\quad Ra_c = 1709.4$

For $Pr = 0.001$ it was difficult to obtain convergence of the solution. The response, Nu vs iteration number (Fig. 13) indicates that Ra_c is around the value 2800.

Table 1. Summary of the computed average Nusselt number for $Pr = 10$

Ra	Nu (6 × 6)	Nu (10 × 10)	Nu (14 × 14)	Nu ($\Delta r \to 0$)
2700	1.8023	1.6338	1.5712	1.495
3700	2.2530	2.0076	1.9008	1.895
4700	2.5509	2.2668	2.1280	1.905
5700	2.7723	2.4679	2.3009	2.057
6700	2.9484	2.6334	2.4431	2.157
7700	3.0948	2.7743	2.5647	2.235
8700	3.2201	2.8991	2.6716	2.340
10 700	3.4267	3.1133	2.8566	2.485
12 700	3.5929	3.2942	3.0120	2.595
14 700	3.7314	3.4509	3.1489	2.750
19 700	4.0003	3.7762	3.4387	2.990
24 700	4.2020	4.0370	3.6746	3.175

Table 2. Summary of the computed average Nusselt number for $Pr = 0.01$

Ra	Nu (10 × 10)	Nu (14 × 14)	Nu (18 × 18)	Nu ($\Delta r \to 0$)
2300	—	1.0142	1.0359	1.067
2400	—	1.0360	1.0605	1.098
2500	1.0161	1.0555	1.0852	1.128
2600	1.0364	1.0798	1.1103	1.158
2700	1.0644	1.1060	1.1405	1.190
2800	1.0924	1.1293	1.1688	1.222
2900	1.1191	1.1616	1.9668	1.245
3000	1.1479	1.1903	1.2231	1.272
3100	1.1840	1.2177	1.2483	1.294
3200	1.2092	1.2441	1.2735	1.315
3300	1.2464	1.2713	1.2976	1.333
3400	1.2745	1.2986	1.3268	1.365
3500	1.3056	1.3246	1.3425	1.370
3600	1.3318	1.3498	1.3725	1.400
3700	—	1.3737	1.3975	1.429
3800	—	1.3978	1.4206	1.452
3900	—	1.4204	1.4425	1.475
4000	—	1.4481	1.4642	1.492

Table 3. Summary of the computed Nusselt numbers for various Prandtl numbers

Ra	Nusselt number (at zero grid size) $Pr = 1.0$	$Pr = 0.1$	$Pr = 0.01$	$Pr = 0.003$
1800	1.054	—	—	—
2000	1.188	1.127	—	—
2200	1.302	1.225	—	—
2300	1.350	1.273	1.062	—
2400	1.396	1.319	1.096	—
2500	1.453	1.363	1.128	—
2600	1.487	1.403	1.156	1.038
2700	1.551	1.442	1.190	1.054
3000	1.645	1.547	1.272	—
3100	—	—	1.293	—
3200	1.726	1.606	1.312	—
3500	—	—	1.380	—
3700	1.832	1.742	1.428	—
4000	—	—	1.492	—
4200	1.923	1.856	—	—

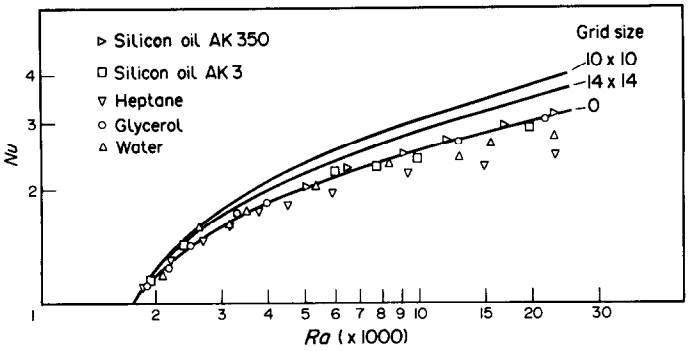

FIG. 7. Comparison of predicted Nusselt number with experimental values of Silveston [16].

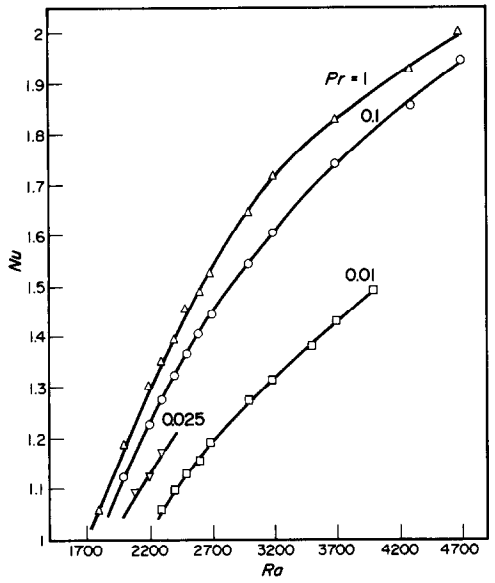

FIG. 8. Influence of Prandtl number on Nusselt number.

5.2. *Correlating equations for the critical Rayleigh number and the heat transfer rate*

A correlating equation developed by Churchill and Usagi [18] was used to generalize the dependence of the critical Rayleigh number on the Prandtl number. The theoretical value 1708 was used as the asymptote for large Pr and C/Pr^b for $Pr \to 0$ with C and b obtained from the values of Ra at $Pr = 0.01$ and $Pr = 0.003$.

The correlating equation

$$(Ra_c)^n = (C/Pr^b)^n + (1708)^n \tag{41}$$

with $C = 1262$ and $b = 0.11$ was found to best represent the data with $n = 28$, yielding

$$(Ra_c)^{28} = (1262/Pr^{0.11})^{28} + (1708)^{28}. \tag{42}$$

Table 4 provides a comparison of the computed values with this correlating equation. The results are also plotted in Fig. 14.

Equation (42) gives a value of $Ra_c = 1708$ for air ($Pr = 0.7$) and 1897 for mercury ($Pr = 0.025$). This latter value is higher than the experimental value of 1808 ± 16 obtained by Verhoeven [4], but within the range observed by Soberman [5].

It is also possible to give a correlating equation for the heat transfer rate near the critical state with using the critical Rayleigh number. The correlating equation can be based on the equation of Malkus and Veronis [17] as shown in equation (40). The constant B is a function of Prandtl number and can be determined from computed data as a gradient of each curve as shown in Fig. 12. These values are fitted again by a correlating equation of Churchill and Usagi [18]. The same method as above gives

$$(B)^{-5} = (1.336)^{-5} + (Pr^{0.312}/0.317)^{-5}. \tag{43}$$

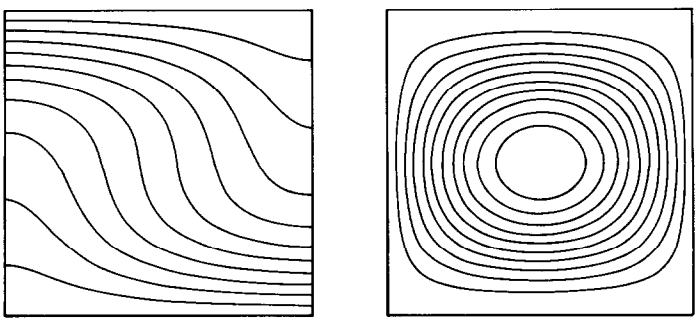

FIG. 9. Computed contours of isotherms and streamfunction at $Ra = 3000$ and $Pr = 10$.

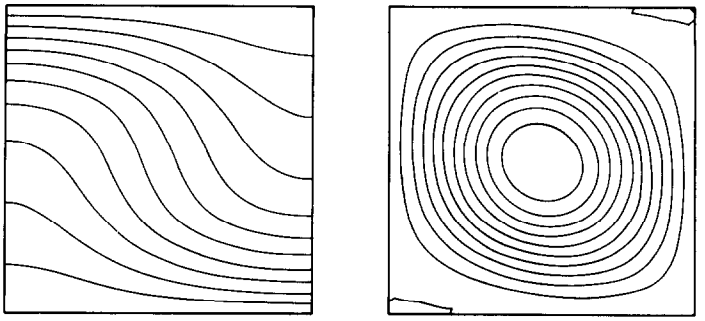

FIG. 10. Computed contours of isotherms and streamfunction at $Ra = 3000$ and $Pr = 0.1$.

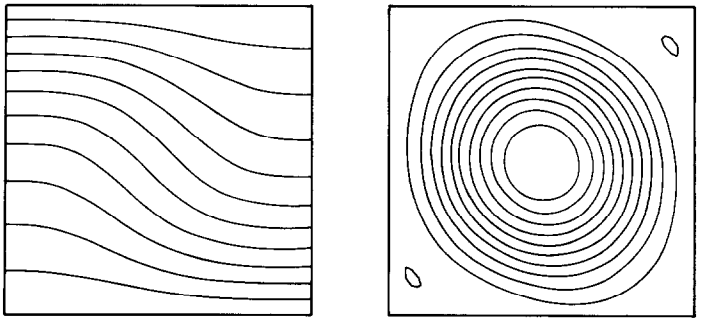

FIG. 11. Computed contours of isotherms and streamfunction at $Ra = 3000$ and $Pr = 0.01$.

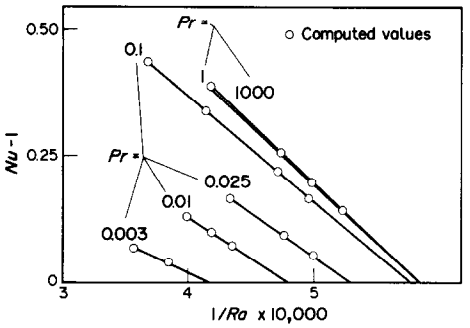

FIG. 12. Determination of critical Rayleigh number for different Prandtl numbers using the equation of Malkus and Veronis.

The corresponding values are reported in Table 5 and plotted in Fig. 15.

6. CONCLUSIONS

Convergent solutions of two-dimensional natural convection in a horizontal fluid layer between two rigid walls heated from below and cooled from above were obtained by the finite-element method.

The computations for $Pr = 10$, agreed well with prior experimental data even for Rayleigh numbers as high as 25 000.

An extrapolation permitted the determination of the critical value of Rayleigh number for low values of Pr.

Table 4. Comparison of the computed critical Rayleigh numbers with other results

	Pr						
	0.001	0.003	0.01	0.025	0.1	1.0	1000.0
Ra_c computed	<2800.0	2392.0	2095.0	1894.0	1721.0	1712.0	1709.0
Ra_c by equation (42)	2698.0	2391.0	2094.0	1897.0	1722.0	1708.0	1708.0
Experimental data [4]				1808 ± 16		1708.0	1708.0
Ra_c [7]	—	—	2242.0	1833.0	1720.0	1708.0	1708.0

Table 5. Comparison of the computed constant B with that by correlating equation (43)

	Pr					
	0.003	0.01	0.025	0.1	1.0	1000.0
B computed	0.480	0.750	0.950	1.210	1.330	1.336
B by equation (43)	0.514	0.741	0.957	1.233	1.332	1.336

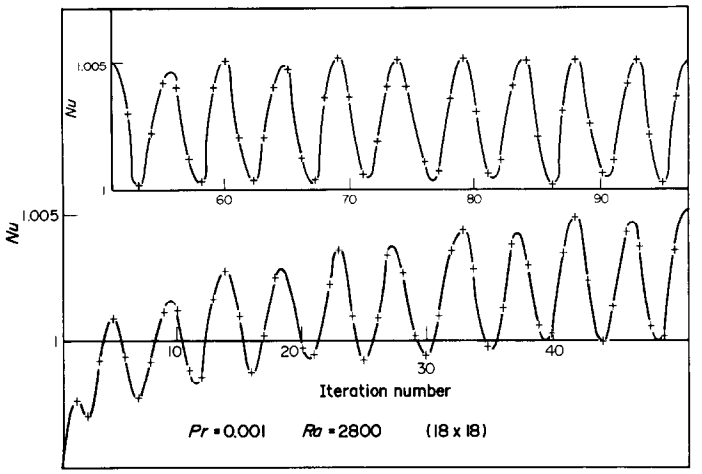

FIG. 13. Nusselt number vs iteration number ($Pr = 0.001$, 18×18 divisions).

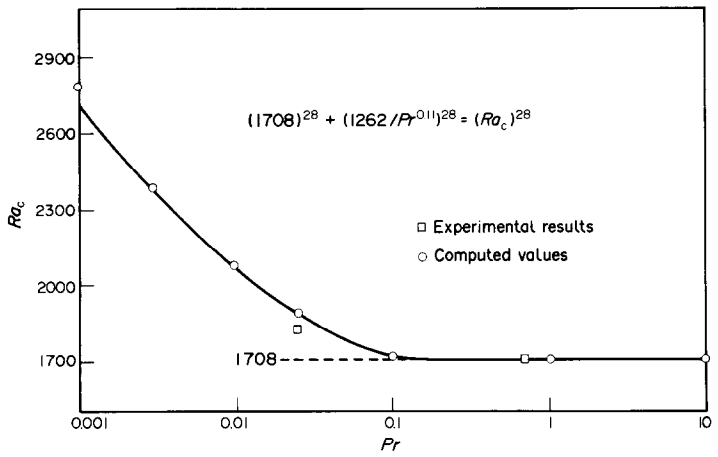

FIG. 14. Correlating equation for critical Rayleigh number: critical Rayleigh number vs Prandtl number.

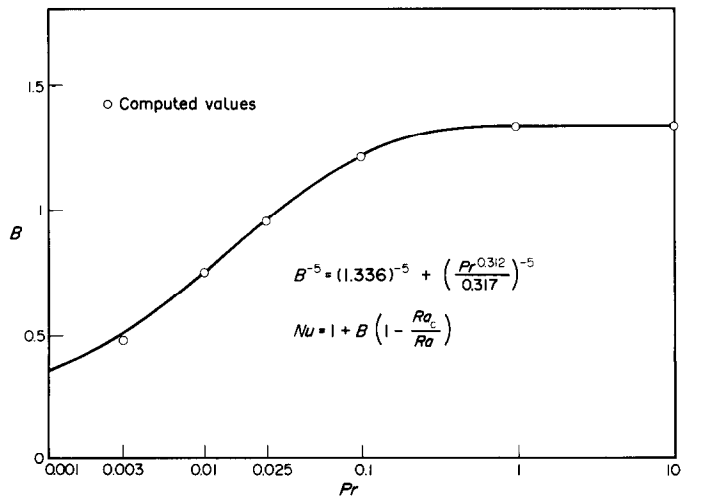

FIG. 15. Correlating equation for Nusselt number near critical state. The constant B, as a function of Prandtl number, corresponds to the equation of Malkus and Veronis.

For such low Prandtl numbers, the viscosity of the fluid is very small and the results obtained correspond to a very large Grashof number, i.e. a very high temperature gradient and high rate of circulation.

Correlating equations were developed for these results, permitting the computation of Nusselt numbers near the critical Rayleigh number for Prandtl numbers as low as 0.001.

Acknowledgements—The stay of H. Bertin at Okayama University was supported by a post-doctoral fellowship program of the J.S.P.S. (Japan Society for the Promotion of Science) from March 1984 to October 1985.The study on the effect of Prandtl number on natural convection was suggested both by Professor T. Fujii, Kyushu University and Professor S. W. Churchill of the University of Pennsylvania, separately more than 10 years ago. We deeply acknowledge their advice. We are also very grateful for the revision in the English text by Professor Churchill.

REFERENCES

1. S. Chandrasekhar, *Hydrodynamic and Hydromagnetic Stability*. Oxford, Oxford University Press (1961).
2. H. Ozoe, K. Fuji, N. Lior and S. W. Churchill, Long rolls generated by natural convection in an inclined, rectangular enclosure, *Int. J. Heat Mass Transfer* **26,** 1427–1438 (1983).
3. E. L. Koshmieder, Bénard convection, *Adv. chem. Phys.* **26,** 177–211 (1974).
4. J. D. Verhoeven, Experimental study of thermal convection in a vertical cylinder of mercury heated from below, *Phys. Fluids* **12,** 1733–1740 (1964).
5. R. K. Soberman, Onset of convection in liquids subjected to transient heating from below, *Phys. Fluids* **2,** 131–138 (1959).
6. M. R. Samuels and S. W. Churchill, Stability of a fluid in a rectangular region heated from below, *A.I.Ch.E. Jl* **13,** 77–85 (1967).
7. P. Chao, S. W. Churchill and H. Ozoe, The dependence of the critical Rayleigh number on the Prandtl number. In *Convection Transport and Instability Phenomena*, edited by J. Zierep and H. Oertel. G. Braun, Karlsruhe (1982).
8. B. Tabarrok and R. C. Lin, Finite element analysis of free convection flows, *Int. J. Heat Mass Transfer* **20,** 945–952 (1977).
9. H. Ozoe, T. Hatano, H. Sayama and S. W. Churchill, Use of the finite element method for natural convection in a horizontally confined infinite layer of fluid, *Numer. Heat Transfer* **6,** 55–66 (1983).
10. M. Ikenouchi and N. Kimura, An approximate numerical solution of the Navier–Stokes equations by Galerkin method. In *Finite Element Methods in Flow Problems*, edited by J. T. Oden *et al.*, pp. 99–100. Pineridge Press, Swansea (1974).
11. A. Moult, D. Burley and H. Rawson, The numerical solution of two-dimensional, steady flow problems by the finite element method, *Int. J. Numer. Meth. Engng* **14,** 11–35 (1979).
12. O. C. Zienkiewicz, *The Finite Element Method*, 3rd edn. McGraw-Hill, New York (1977).
13. T. J. Chung, *Finite Element Analysis in Fluid Dynamics*. McGraw-Hill, New York (1978).
14. A. J. Baker, *Finite Element Computational Fluid Mechanics*. Hemisphere, Washington, DC (1983).
15. S. W. Churchill, P. Chao and H. Ozoe, Extrapolation of finite differences calculations of laminar natural convection in enclosures to zero grid size, *Numer. Heat Transfer* **4,** 39–51 (1981).
16. P. L. Silveston, Wärmedurchgang in wärgerechten flüssigkeitsschichten, *Forsch. Ing.* **24,** 59–69 (1958).
17. M. V. R. Malkus and G. Veronis, Finite amplitude cellular convection, *J. Fluid Mech.* **4,** 225–260 (1958).
18. S. W. Churchill and R. Usagi, A general expression for the correlation of rates of transfer and other phenomena, *A.I.Ch.E. Jl* **18,** 1121–1128 (1972).

ETUDE NUMERIQUE PAR LES ELEMENTS FINIS DE LA CONVECTION NATURELLE BIDIMENSIONNELLE DANS UNE COUCHE FLUIDE HORIZONTALE CHAUFFEE PAR LE BAS: INFLUENCE DU NOMBRE DE PRANDTL

Résumé—La convection naturelle dans une couche fluide horizontale chauffée par les bas et refroidie par le haut est traitée par une méthode d'éléments finis utilisant une approche Galerkin. Dans le cas $Pr = 10$, le nombre de Nusselt, obtenu par une extrapolation à la taille d'élement nulle, s'accorde bien avec les données expérimentales de Silveston [Forsch. Ing. **24,** 54–69 (1935)], pour un domaine de nombres de Rayleigh depuis la valeur critique jusqu'à 25 000. Pour les nombres de Prandtl variant de 0,001 à 1 000, les solutions permanentes des transferts thermiques et des nombres de Rayleigh critiques sont calculés. On propose une équation du nombre de Rayleigh en fonction du nombre de Prandtl. Utilisant l'équation de Malkus et Veronis [*J. Fluid Mech.* **4,** 225–260 (1953)], il est possible de calculer le flux de chaleur près de l'état critique pour chaque nombre de Prandtl supérieur à 0,001.

NUMERISCHE UNTERSUCHUNG DER ZWEIDIMENSIONALEN NATÜRLICHEN KONVEKTION IN EINER VON UNTEN BEHEIZTEN HORIZONTALEN FLUIDSCHICHT MIT DER METHODE DER FINITEN ELEMENTE: EINFLUSS DER PRANDTL-ZAHL

Zusammenfassung—Die zweidimensionale natürliche Konvektion in einer von unten beheizten und von oben gekühlten horizontalen Fluidschicht wurde mit einer Methode der finiten Elemente unter Anwendung einer Galerkin-Näherung berechnet. Für $Pr = 10$ und Rayleigh-Zahlen im Bereich vom kritischen Wert bis zu 25000 stimmt die durch Extrapolation der Elementgröße auf Null erhaltene Nusselt-Zahl sehr gut mit den experimentellen Daten von Silveston [*Forsch. Ing.* **24,** 59–69 (1985)] überein. Für Prandtl-Zahlen von 0,001 bis 1000 wurden stationäre Lösungen für Konvektion, Wärmeströme und kritische Rayleigh-Zahlen berechnet. Eine Korrelationsgleichung für die kritische Rayleigh-Zahl wurde als Funktion der Prandtl-Zahl vorgeschlagen. Mit Hilfe der Korrelations-Gleichung von Malkus und Veronis [*J. Fluid Mech.* **4,** 225–260 (1953)] war es möglich, den Wärmestrom nahe des kritischen Zustandes für Prandtl-Zahlen größer als 0,001 zu berechnen.

ЧИСЛЕННОЕ ИССЛЕДОВАНИЕ МЕТОДОМ КОНЕЧНЫХ ЭЛЕМЕНТОВ ПЛОСКОЙ ЕСТЕСТВЕННОЙ КОНВЕКЦИИ В ГОРИЗОНТАЛЬНОМ СЛОЕ ЖИДКОСТИ, НАГРЕВАЕМОМ СНИЗУ. ВЛИЯНИЕ ЧИСЛА ПРАНДТЛЯ

Аннотация—Естественная конвекция в горизонтальном слое жидкости, нагреваемом снизу и охлаждаемом сверху, рассчитывается методом конечных элементов с использованием метода Галеркина. В случае $Pr = 10$ число Нуссельта, полученное экстраполяцией к нулю размера элемента, хорошо согласуется с экспериментальными данными Сильвестона для широкого диапазона чисел Рэлея от критического значения до 25000. Для чисел Прандтля, изменяющихся от 0,001 до 1000, получены стационарные решения для структуры конвекции, коэффициенты теплообмена и критические числа Рэлея. Предложено соотношение для расчета критического числа Рэлея в зависимости от числа Прандтля. С помощью корреляции Малкуса и Вероника оказалось возможным найти коэффициент теплообмена вблизи критического значения числа Рэлея.